LAWRENCE
LIVERMORE
NATIONAL
LABORATORY

LLNL-CONF-555292

X-ray bang-time and fusion reaction history at ~ps resolution using RadOptic detection

S. P. Vernon, M. E. Lowry, K. L. Baker, C. V. Bennett, J. R. Celeste, C. Cerjan, S. Haynes, V. J. Hernandez, W. W. Hsing, R. A. London, B. Moran, A. Schach von Wittenau, P. T. Steele, R. E. Stewart

May 4, 2012

X-ray bang-time and fusion reaction history at ~ps resolution using RadOptic detection
Monterey, CA, United States
May 6, 2012 through May 10, 2012

Disclaimer

X-ray bang-time and fusion reaction history at ~ ps resolution using RadOptic detection[a)]

S.P. Vernon [b)], M.E. Lowry, K.L. Baker, C.V. Bennett, J.R. Celeste, C. Cerjan, S. Haynes, V.J. Hernandez, W.W. Hsing, R.A. London, B. Moran, A. Schach von Wittenau, P.T. Steele, R.E. Stewart

Lawrence Livermore National Laboratory, P.O. Box 808, Livermore CA 94551-0808, USA

(Presented XXXXX; received XXXXX; accepted XXXXX; published online XXXXX)

We report recent progress in the development of RadOptic detectors, radiation to optical converters, that rely upon x-ray absorption induced modulation of the optical refractive index of a semiconductor sensor medium to amplitude modulate an optical probe beam. The sensor temporal response is determined by the dynamics of the electron-hole pair creation and subsequent relaxation in the sensor medium. Response times of a few ps have been demonstrated in a series of experiments conducted at the LLNL Jupiter Laser Facility. This technology will enable x-ray bang-time and fusion burn-history measurements with ~ ps resolution.

I. Introduction

Prompt measurement of fusion burn at the National Ignition Facility will require detection systems with a temporal resolution of 1ps or better. Conventional x-ray (and other ionizing radiation) detectors collect the charge generated by the interaction of the incident radiation with the sensor medium and generate currents or voltages that are transported, usually via signal cables, to remote recorders. The degradation of the high frequency signals components during signal generation and transmission limits the temporal response of state-of-the-art electronic detection systems to, at best, tens of ps. RadOptic detection systems overcome these limitations by detecting the radiation induced charge distribution in place, the sensor (typically a II-VI or a III-V semiconductor alloy), produces a phase modulation of an optical probe beam interrogating the sample. The amplitude of modulation is proportional to radiation intensity. Since no charge transport is required, RadOptic sensors are inherently high-bandwidth and sensor temporal response is determined by the charge carrier equilibration and relaxation times. There are multiple approaches to the detection and recording of the phase modulated optical probe beam.

For example, Mach-Zehnder[1] and Fabry-Perot[2] sensors employ interferometric detection. The charge generated by radiation absorption within the sensor medium modifies the sensor medium optical refractive index; the change in refractive index alters the optical reflectivity of (or optical transmission through) the sensor material, modulating the phase of the reflected (or transmitted) optical probe. Interferometric analysis of the reflected (or transmitted) optical beam produces a modulation of the beam amplitude. In effect the radiation signal is "down-converted" to an amplitude modulated optical beam.

A complementary approach, diffractive detection, requires an impressed periodic, spatial modulation of the incident radiation signal produced, for example, by inserting a transmission grating between the radiation source and the sensor[3]. The impressed spatial modulation of the transmitted beam induces a phase grating in the sensor medium. A probe beam incident on the sensor is diffracted by the phase grating and can be separated into various orders, spatially filtered and collected by an optical imaging system to produce an optical replica of the x-ray image[4].

I. Introduction

We have previously shown that an xray signal can induce an optical phase shift[1] of a probe beam in a semiconductor given by[5]

$$\phi(t) = \int_{-\infty}^{\infty} S(t)\kappa f(t-\tau)d\tau \quad . \qquad (1)$$

Where *S(t)* is the absorbed radiation energy fluence (keV/μm^2/ps), κ is a sensitivity parameter, and *f(t)* is a response function of the material. It is important to realize that this leads to a detector response which is independent of detector area, making this approach well-suited to imaging applications[2,3,4]. The material response function is given by[5],

$$f(t) = \frac{e^{-t/\tau_r}}{\eta}\left[1 - e^{-\eta t/\tau_g}\right] \qquad (2)$$

Where τ_g is the time it takes to generate effective electron-hole (*e-h*) pairs, τ_r is the time it takes for these to recombine, and $\eta = 1 - \tau_g/\tau_r$. Eq. (2) is plotted in fig. 1 for several values of the e-h pair recombination time. The detectability of the phase signal *ϕ(t)* scales with the peak amplitude of *f(t),* thus there is a fundamental tradeoff between detectability (or sensitivity) and impulse response. We also note that the peak amplitude of *f* is a strong decreasing function of the ratio, τ_g/τ_r .

[a)]Contributed paper published as part of the Proceedings of the 19th Topical Conference on High-Temperature Plasma Diagnostics, Monterey, California, May, 2012.
[b)]Author to whom correspondence should be addressed: vernon1@llnl.gov.

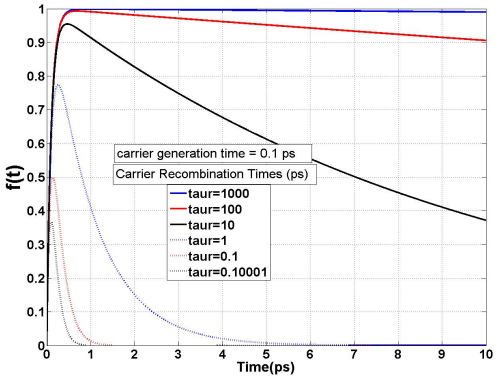

Figure 1. RadOptic material response function

It is useful to consider two important limiting cases: the integrating detector and the impulsive detector. The integrating case results when τ_r is large compared to S(t) timescales, thus the response function can be approximated by the Heaviside function.

$$f(\tau)=\theta(\tau) \quad \phi(t)_{integrating} = \kappa \int_{-\infty}^{t} S(\tau)\,d\tau \qquad (3)$$

The case of impulsive detector is given by

$$\phi(t)_{impulsive} = \int_{-\infty}^{\infty} S(t)\hat{\kappa}_f \delta(t-\tau)\,d\tau = \hat{\kappa}_f S(t)\ , \qquad (4)$$

where $\hat{\kappa}_f = \kappa \int_{-\infty}^{\infty} f(\tau)_{impulse}\,d\tau = \kappa\tau_r$.

In the case of the integrating detector, *S(t)* may be recovered by differentiation of $\phi(t)_{integrating}$. The impulse response of this differentiated signal will be governed by τ_g. While the differentiation operation necessarily adds noise and degrades the SNR, the integrating detector offers a better SNR than the impulsive detector. We are continuing to investigate the comparative SNR characteristics of the differentiated integrating detector and the corresponding impulsive detector, but thus far they appear to be nearly equivalent.

III. RadOptic X-ray Detection

Recent experiments measured the relative sensitivity and SNR of Fabry-Perot cavities (radsensors) operated as integrating and impulsive x-ray detectors (results in figs 2 and 3, respectively). As discussed above the Fabry-Perot converts the phase modulation of the probe to amplitude modulation. There are several possible recording options.

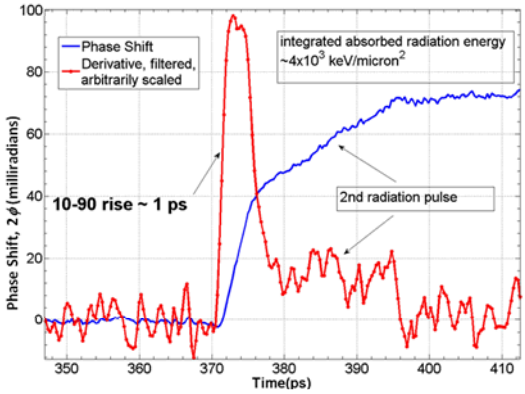

Figure 2. Integrating RadOptic detector response.

The Callisto laser at LLNL's Jupiter Laser Facility, operating at 800 nm with 60fs optical pulses, shooting 12.5 micron Cu targets, provided ~8keV Cu-K_α radiation, lower energy bremsstrahlung, and high energy electrons absorbed within the radsensors. The radsensor detectors had an active region of epitaxially grown InGaAsP. The "impulsive" detector had an optically measured τ_r ~3ps, due to the introduction of trapping centers by ion bombardment. The "integrating" detector active region was as-grown epi. We used the recently developed TimeLens[6] recording system which has an ~1ps impulse response. Alternative fast recording schemes include the all-optical streak camera, SLIDER[7].

The xray level for the impulsive detector, fig. 3 was ~x100 higher than for the integrating detector, fig. 2, making the better sensitivity of the integrating detector apparent. Both detectors captured similar double-pulse features.

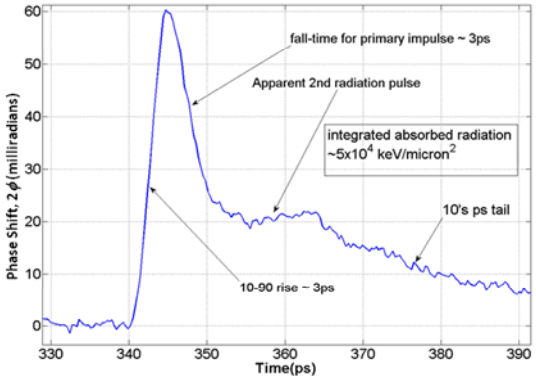

Figure 3. Impulsive RadOptic detector response

Although absolute xray sensitivity calibrations at short pulse laser facilities are difficult, the estimated sensitivity from these measurements is κ=0.01 milliradians/keV/μm^2.

In fig. 4 an optical replica of an x-ray image, recorded using a diffractive imaging technique. The image was produced by illuminating a slab of CdSe with Ti K_α x-rays propagated through a lithographically formed transmission mask and generated using an LPP source driven by the Callisto short pulse Ti:sapphire laser system at JLF/LLNL,. The two images correspond to the orthogonal polarization states of an optical probe beam; the temporal delay between polarizations is ~ 5 ps. The sequential,

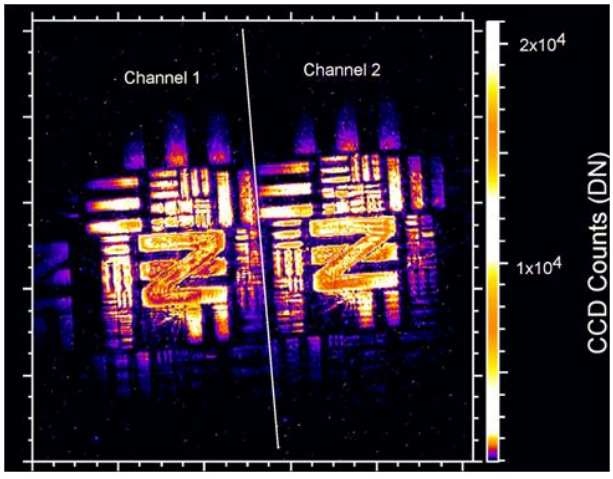

Figure 4. Diffractive imaging.

time-separated images are, in effect, a two frame x-ray movie with an effective frame rate of $2x10^{11}$ frames per second.

IV. RadOptic X-ray Bang Time and Reaction History

High-speed xray detection is useful for the precise measurement of xray bang time as well as the measurement of xray reaction history for advanced burn diagnostics. Our NIF deployment of the RadOptic Diagnostic-Bang Time (ROD-BT) has two phases: An early deployment using a fast-photodiode and scope to measure the amplitude modulated radsensor output (18 ps response capability), followed by a second phase using the TimeLens recording system (1-2 ps system response capability).

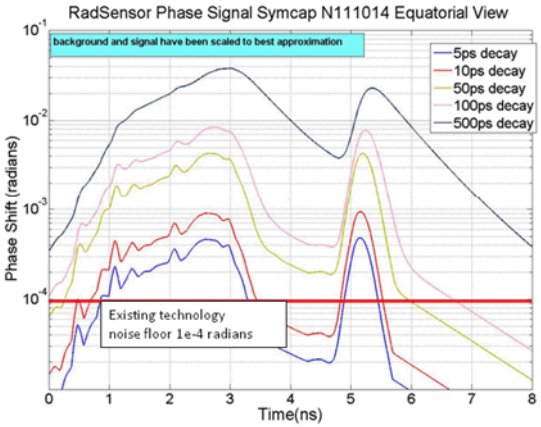

Figure 5. RadSensor/Scope simulated signals.

Figure 5, displays some of our system modeling results for the phase 1, scope-based system, where we compare the expected signal level for radsensor detectors with various values of device recovery time τ_r. The plots show the expected phase shift for an xray signal from a particular capsule, Symcap N111014. The xray signals are simulations, which include the hohlraum background (the early-time, long-duration pulse) and the capsule self-emission (the shorter, later pulse). The detector simulation assumed a 20 micron Ge xray filter and a RadSensor active layer of 4.09 microns of InGaAsP, positioned 50 cm from TCC. The noise floor of 100 microradians is due to scope noise, shot noise, and our existing radsensor cavity technology.

V. RadOptic Nuclear Detection

Direct RadOptic detection of fusion neutrons, *n*, and gamma, γ, rays is made difficult by the relatively low interaction cross sections of *n* and γ with solid state materials. Efficient detection requires conversion of the incident radiation to ~ 20 keV electrons which interact strongly with the semiconductor sensor. Conversion losses can be overcome using an electron optical system to concentrate the electron flux onto the sensor. The success of this contingent upon two factors: 1) affecting the *n-e* or γ-*e* conversion with ~ ps temporal dispersion and 2) low ~ ps temporal dispersion propagation of the electron flux onto the sensor.

As illustrated in fig. 6, the *n* converter concept utilizes a CsI coated plastic foil to convert recoil protons into secondary electrons, the γ converter concept utilizes pair production in a W slab, Cherenkov radiation in LiF and secondary electron generation in CsI to produce the secondary electron flux. MCNP

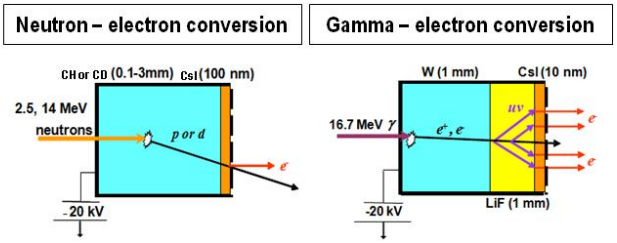

Figure 6. Converter concepts.

and GEANT simulations of the converter response indicate that conversion at ~ ps temporal resolution is achievable for both designs. Validation of the electron transport and RadOptic electron detection concept is in progress using a laser driven photocathode as a surrogate for the electron emission.

VI. Conclusions

The RadOptic approach provides a versatile solution for high bandwidth detection of radiation. Down conversion of the radiation signatures to a modulated optical probe circumvents problems arising from charged particle transport and signal propagation and enables recording of radiation signals with ~ ps temporal resolution. A variety of RadOptic sensor architectures have been demonstrated and the technique naturally lends itself to single channel detectors and multi-channel imaging. Extensions of the technology to the problem of fusion burn history, and the direct detection of n and g rays is in process.

VII. Acknowledgements

We are grateful to Alan Szu-hsin Wan and Cynthia K. Nitta for their encouragement and support. This work was performed under the auspices of the U.S. Department of Energy by Lawrence Livermore National Laboratory under Contract No. DE-AC52-07NA27344.

---

[1] M.E. Lowry, C.V. Bennett, S.P. Vernon, T. Bond, R. Welty, E. Behymer, H. Petersen, A. Krey, R. Stewart, N.P. Kobayashi, V. Sperry, P. Stephan, C. Reinhardt, S. Simpson, P. Stratton, R. Bionta, M. McKernan, E. Ables, L. Ott, S. Bond, J. Ayers, O.L. Landen, and P.M. Bell, Proc. SPIE **5194**, pp. 193-204. (2004).
[2] M.E. Lowry, C.V. Bennett, S.P. Vernon, R. Stewart, R.J. Welty, J. Heebner, O.L. Landen, P.M. Bell, Rev. Sci. Instrum. **75**, 3995 (2004).
[3] K.L. Baker, R.E. Stewart, P.T. Steele, S.P. Vernon and W.W, Hsing, to be submitted to APL (2012).
[4] R.E. Stewart, P.T. Steele, K.L. Baker, S.P. Vernon and W.W. Hsing, to be submitted to RSI (2012).
[5] M.E. Lowry, S.P. Vernon, P.T. Steele, C.V. Bennett, V.J. Hernandez, B. Moran and S. Haynes, Proc. UltraFast Optics VIII, pp. 225-226, Monterey (2011).
[6] Hernandez, V. J., Bennett, C. V., Moran, B. D., Drobshoff, A. D., Langrock, C., Chang, D., Fejer, M. M., and Ibsen, M. (2009) "745 fs Resolution Single-shot Recording at 2.1 TSample/s and 104 Mframes/s Using Temporal Imaging," OSA Nonlinear Optics Conference, Honolulu, HI, July 17, 2009, Paper PDNFA2.
[7] C. H. Sarantos and J. E. Heebner, "Solid-state ultrafast all-optical streak camera enabling high-dynamic-range picosecond recording," Opt. Lett., **35**, pp. 1389-1391,(2010).